Article

Damage Accumulation in the Hybrid Composite Material Reinforced by Oil Shale Ash (OSA) Powder and 3D-Knitted Fabric Subjected to Mechanical Loading

Olga Kononova , Andrejs Krasnikovs * , Umesh Haribhai Vavaliya * , Arturs Macanovskis , Inga Lasenko , Karunamoorthy Rengasamy Kannathasan , Ilgar Jafarli , Iveta Novakova , Riho Motlep , Mindaugas Vaishnoras

Posted Date: 23 February 2024

doi: 10.20944/preprints202402.1294.v1

Keywords: hybrid composite material; oil shale ash; knitted fabric; thread failure

Article

Damage Accumulation in the Hybrid Composite Material Reinforced by Oil Shale Ash (OSA) Powder and 3D-Knitted Fabric Subjected to Mechanical Loading

Olga Kononova [1], Andrejs Krasnikovs [1,*], Umesh Haribhai Vavaliya [1], Arturs Macanovskis [1], Inga Lasenko [1], Karunamoorthy Rengasamy Kannathasan [1], Ilgar Jafarli [1], Iveta Novakova [2], Riho Mõtlep [3] and Mindaugas Vaishnoras [4]

[1] Department of Theoretical Mechanics and Strength of Material, Institute of Mechanics and Mechanical Engineering, Riga Technical University, LV-1048 Riga, Latvia; olga.kononova@rtu.lv (O.K.); Umesh-Haribhai.Vavaliya@rtu.lv (U.H.V.); arturs.macanovskis@rtu.lv (A.M.); inga.lasenko@rtu.lv (I.L.); karunamoorthy.rengasamy-kannathasan@rtu.lv (K.R.K.)

[2] Department of Construction, Energy and Material Technology, The Arctic University of Norway, Lodve Langesgate 2, 8514, Narvik, Norway; iveta.novakova@uit.no

[3] Institute of Ecology and Earth Sciences, University of Tartu, Juhan Liivi 2, 50409 Tartu, Estonia; riho.motlep@ut.ee

[4] Lithuanian Energy Institute, Breslaujos st. 3, LT-44403, Kaunas, Lithuania; mindaugas.vaisnoras@lei.lt

* Correspondence: andrejs.krasnikovs@rtu.lv

Abstract. Hybrid reinforcement in a composite material (CM), in many situations, allows better govern material mechanical properties. Polymer matrix CM plate is reinforced with small particles and macro-fibers. Particles are oil shale ash (OSA) powder, macro-fibers – basalt fiber threads impregnated by matrix material. With the goal to find out elastic properties of the matrix- polymer with OSA, samples with its different concentrations were experimentally fabricated and their elastic properties were experimentally measured. Obtained data were used in numerical modelling. Was observed polymer matrix composite slab, reinforced with OSA and three-dimensional (3D) basalt fiber fabric. Fabric are forming threads impregnated by matrix (polymer resin mixed with OSA particles). Damage accumulation in the stretched slab was modelled. Impregnated thread, in the modelling, is observed as a macro-fiber (MF) with averaged elastic properties. With the load increase MF in the material began to break. At first, appeared isolated single breaks. A probabilistic sequential MF rupture accumulation model was accepted and numerically realized. The geometry of the reinforcing knitted fabric was modeled using the Leaf and Glaskin approach. In the knitted fabric highly, stressed MF cross-sections are observed as potential location where thread breakage can occur. If one thread breaks, the cross-sections of the adjacent threads experience the overload caused by this rupture. More overloaded crossection in the adjacent overloaded thread breaks and we obtain two adjacent broken MF designated as a defect with the size j=2. The probabilities of obtaining defect consisting of at least $2, 3, \ldots j$ adjacent broken MF in the plate were calculated. The calculations continued until the rupture process becomes unstable ($j \to \infty$). The overstresses on adjacent threads in the CM were calculated using the FEM three-dimensional numerical approach. Analytical and stochastic methods were used for the load-carrying capacity determination and different size defects accumulation in the hybrid composite material (HCM) plate. Also, was calculated the probability of the plate rupture.

Keywords: hybrid composite material; oil shale ash; knitted fabric; thread failure

 doi:10.20944/preprints202402.1294.v1

1. Introduction

Nowadays, interest in composite materials with hybrid reinforcement (CMHR) jointly working in one material is increasing for a few reasons. One is economical: it allows to create composites with synergetic properties [1–6], second - ecological, important for our investigation: is possible to fabricate "green" composites utilizing cheap or "waste" materials (in our situation OSA powder) as one of reinforcements in CMHR. And third is mechanical: addition of different concentrations of small particles (is possible to use powders of milled sand, fly ash, nano-clay, OSA, etc.) allows to modify elastic properties of the matrix and to manage the mechanical cracking process. Interest for such materials in different engineering applications is growing [7–9]. In the present research we investigate a textile reinforcement as the main loadbearing element in the CMHR. CMHR material has relatively low fabrication cost and has advantages in terms of its textile reinforcement topology. Textile-reinforced composites can replace numerous currently using metallic products in a range of structural applications. At the same time, in many cases, textile-reinforced composites are also competitive with those that are traditionally fabricated, which use prepregging, layer stacking, and autoclave manufacturing methods. Traditionally fabricated layered composites, with unidirectionally oriented fibers in plies, are characterized by relatively low tensile and shear strength in the direction orthogonal to fibers in plies and in the thickness direction, leading to the accumulation of cracks in the plies, as well as low wearability, impact resistance, and sometimes damage tolerance [10–14]. One promising direction in textile-reinforced composite fabrication technology is the use of knitted fabrics [7,15–17]. The main advantage of such reinforcement is the possibility to produce products with complex shapes without having gaps in reinforcement at the stage of material fabrication. This follows from the loose structure of looped material, which enables the fabric to have relatively large stretch deformation when adapting to complicated shapes [17–19]. In general, two types of knitting can be applied. Warp and weft knits, which have enhanced properties in certain directions, can be used as reinforcement for composite materials. The present investigation explores one of them, weft-knitted reinforcement [7,16,21]. Composite material (CM) with such reinforcement exhibits high energy absorption and impact resistance. Comparing to woven fabric, in the case of knitted fabric, the strands form loops. The fabric is highly deformable in all directions, because the yarns do not make any straight lines anywhere in the material [21,22]. Under applied mechanical loads, composite material accumulates damage. The failure scenario is quite different in situations where the matrix is a polymer (exhibiting elasto-plastic behavior) or ceramic/concrete (exhibiting brittle-elastic behavior). When micro powder is added to the polymer matrix (in our investigation OSA), the matrix becomes stiffer. A matrix with a very high concentration of OSA leads to a failure scenario change in terms of the material; magistral cracks appear, bridged by textile yarns. Such materials are out of the framework of present investigation. The numerical analysis in the present paper was performed for polymer (epoxy resin) matrix containing different concentrations of added OSA in a dispersed form and knitted basalt fiber textile. The material had basalt fiber yarns, which are easily twisted and impregnated with the matrix [23,24]. Textile HCM strength and failure mechanisms depends on hybrid matrix mechanical properties. Applied external stretching load is leading to disperse threads (MF) rupture site accumulation in CMHR volume. Raptured MF place is forming small defect-crack in the CM. In the present investigation we accept that MF rapture happen orthogonally to its longitudinal axis. Two broken crossections in two adjacent macro-fibers are forming double big defect, three - triple big and etc.

Existing polymer matrix with textile-reinforced composite failure models are mainly based on different phenomenological criteria [8,25–27]. Approaches exploiting probabilistic models [28–33] allow to investigate local damage accumulation process in composites, at the same time, majority of them are focused on unidirectional fiber materials. Results obtained for textile HCM would be interesting for better such materials failure picture understanding. These problems are not enough investigated.

 doi:10.20944/preprints202402.1294.v1

2. Materials

OSA is a powder having particles size starting with hundreds of *n*m to hundreds of μm. OSA is classified as industrial waste produced in Estonia due to oil shale mining, processing and burning. Ecologically important is to use OSA in different products.

2.1. Matrix

OSA in concentrations from 0% to 20% was added to liquid epoxy resin. The mixtures were properly mixed, and samples according to the standard ISO 527-2 1B-1 were cast (see Figure 1a,b). After maturing, each sample was polished, stickers with lines were glued, the sample was fixed in testing machine grips, and the elastic modulus was measured. Fully automated testing machine Zwick Roell Z150 was used for applied force determination. Deformation was measured using video extensometer Messphysik (Measurements corresponded to grade 0.5/1 according to standards DIN EN ISO 7500-1 (DIN 51220, DIN 51302), ISO R147, ASTM E4). Measurements were done according to standart ISO 527-2. Experimental data (average over 6 samples) are shown in the Table1. Poisson's ratio for epoxy resin was obtained from the literature and that for epoxy matrix with OSA was calculated using simple averaging formulas (see in the paper Kaw [34]).

Figure 1. Fabrication of epoxy resin with OSA samples: (a) casting; (b) sample in a mold; (c) sample ready for testing; d) mechanical testing.

2.2. Textile

Second HCM reinforcement is knitted fabric. Threads consisting of basalt microfibers were impregnated with the epoxy resin with OSA without forming internal visual voids or cavities. As was mentioned above we are designating the single impregnated thread as a composite macrofiber (MF). Basalt fiber mechanical properties were obtained from supplier and MF elastic properties were calculated by averaging over MF volume.

3. Numerical Damage Accumulation Modeling in Composite Plate Reinforced by Knitted Fabric

In numerical calculations we accepted, HCM has elastic matrix reinforced by knitted fabric made out of MF. Structural damage accumulation model is consisting of two parts. Part one – numerical model of damage accumulation and part two – calculation method how growing defects in the material are forming overstresses in the material volume around them.

3.1. Stress Distribution in the CMHR. Assumptions

We assume MF is isotropic, its elastic constants are obtained by averaging over volume. HCM plate is stretched in one direction. According to stochastic failure nature, load increase is leading to single broken MF sites accumulation in the plate. Each such single isolated breakage is designated as a defect with the size j=1. Failure is observed as the sequential rupture of yarn loops (MF) in the material due to increasing overstress on the MF located around the defect. In the model, more heavily overloaded by stretching stress MF orthogonal crossection, (along its length) is potential place for overloaded neighbor's failure. In the works of other researcher [8,25–27] polymer matrix- textile-

 doi:10.20944/preprints202402.1294.v1

reinforced composite failure was modeled using different phenomenological approaches. Compared with them, this approach is structural. The structural approach can give new information about internal failure mechanisms in materials with sophisticated internal structure and create recipes for material properties improvement. The plate reinforced by single-in plane knitted fabric. Observing a single-layer plate, the plate is stretched by acting in-plane loads. The matrix material is epoxy resin with OSA, and the reinforcement is weft-knitted fabric impregnated with basalt fiber yarns. It should be mentioned that ideologically similar modeling can be used for HCM with other types of polymer matrix with other than OSA powder filler and synthetic fiber threads.

In the framework of our calculations, the composite matrix material (epoxy resin with OSA) is elasto-plastic. The addition of OSA is changing the matrix behavior to more brittle. Deformation till crack formation is decreasing. For highly brittle matrix calculation model must be changed, because matrix cracks formation will play initial role. Basalt fiber yarn impregnated by composite resin is observed as a "large" diameter fiber, macrofiber with elastic properties that are calculated according to the rule of mixture [27,34]. Such fiber is accepted as elastic until its rupture. The elastic properties of the matrix and reinforcement (MF) material are shown in the Table 1.

Table 1. Elastic properties of matrix with OSA.

	Matrix with epoxy resin and 0% (weight) OSA	Macrofiber- basalt fiber thread impregnated by epoxy resin and 0% (weight) OSA
Density ϱ (g/cm^3)	1.19	1.74
Young's modulus E (GPa)	3.15	63.4
Poisson's ratio ν	0.35	0.3
	Matrix with epoxy resin and 10% (weight) OSA	Macrofiber- basalt fiber thread impregnated by epoxy resin and 10% (weight) OSA
Density ϱ (g/cm3)	1.26	1.89
Young's modulus E (GPa)	3.28	63.5
Poisson's ratio ν	0.34	0.29
	Matrix with epoxy resin and 20% (weight) OSA	Reinforcement with basalt fiber thread in epoxy resin and 20% (weight) OSA
Density ϱ (g/cm^3)	1.34	2.07
Young's modulus E (GPa)	3.62	64.1
Poisson's ratio ν	0.33	0.28

The geometric model for the HCM reinforced by the plain weft-knitted fabric is shown in Figure 2. This structure is loaded. The constant displacement is applied in horizontal direction, as is shown in Figure 3. Surface C is not moving in horizontal direction, surface B in vertical. The structure was numerically analyzed (using FEM) for prediction of the sequential yarn failure progress. The main parameters of the knitted fabric geometry are as follows: macrofiber diameter d = 0.55 mm; wale number W = 1.43 loop/cm, which is defined as the number of repeating loops per unit length along the course direction; and course number C = 2.5 loops/cm, which is the number of loops per unit length in the wale direction. Leaf and Glaskin's geometrical model was also used in [6,15,19,24,25].

 doi:10.20944/preprints202402.1294.v1

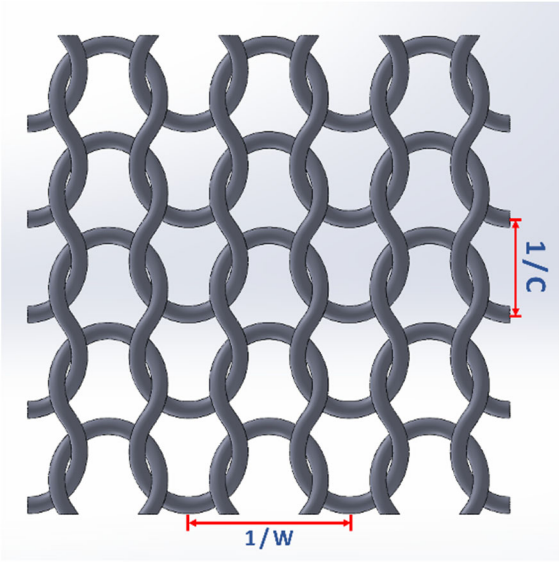

Figure 2. Reinforcement geometry.

The geometric parameters of the investigated composite material plate were as follows: width 21 mm, height 20 mm, and thickness 2.43 mm (Figures 2 and 3). Observed Epoxy resin is elasto - plastic material with tensile yield stress equal to 30 MPa. In the Figure 3a is possible to see the FEM mesh for whole HCM plate and meshed macrofibers which are forming the textile spatial structure inside the HCM plate.

With the goal to optimize calculation time and diminish boundary conditions effect on overstress calculation, the same model was used with the elastic frame (two plates with similar width as for the structural model). Plates (frame) had the averaged, homogenized HCM elastic properties. Figure 4 shows the model with the frame. All loops and the matrix between them were meshed. Perfect bonding conditions were applied between matrix and the outer surface of each macrofiber (without delaminations and voids).

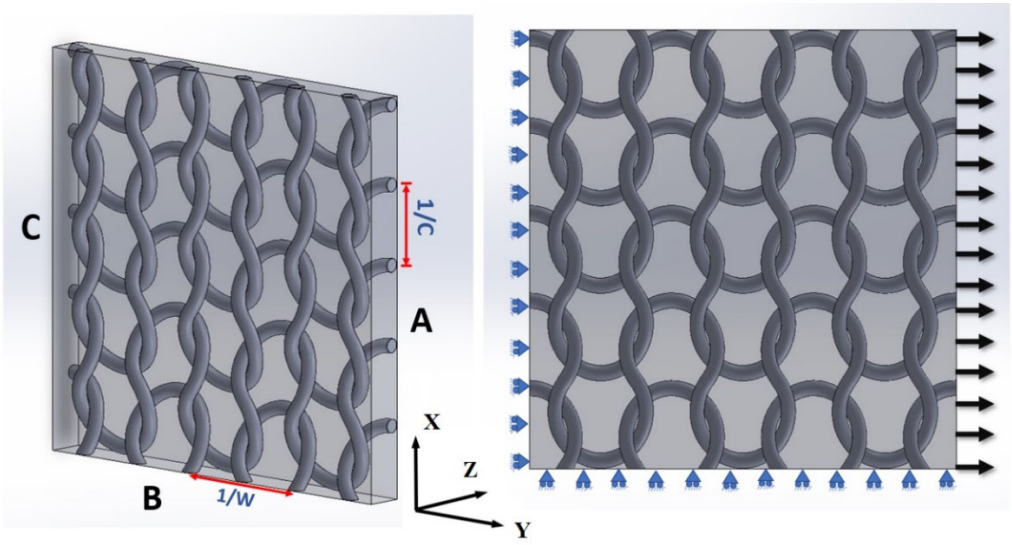

Figure 3. Boundary conditions for HCM volume without the frame.

 doi:10.20944/preprints202402.1294.v1

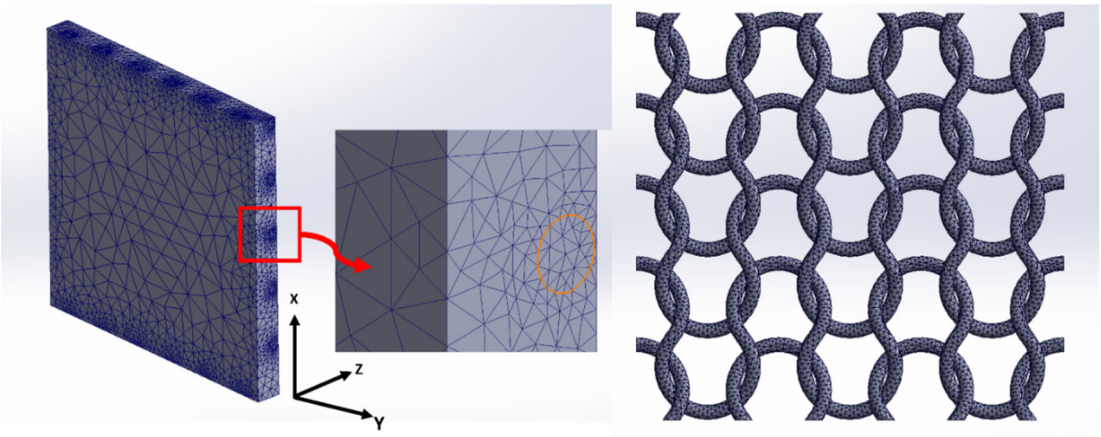

(**a**) (**b**)

Figure 3. A. Mesh for HCM (Matrix and fiber) volume without the frame; a) meshed matrix and macrofibers; b) meshed macrofibers.

Side plane ABC remained planar during the whole loading process. Nodes on the butt-end surface C were fixed in the y direction, and points on surface B could not move in the x direction. Another butt-end surface A obtains displacement Δ_y. External stretching raised a non-equal stress distribution in the yarn loops (MF) that form the material reinforcement. Finite element analysis was carried out for this plate and results for the model with the frame are shown in Figure 5. In the Figure 5 is possible to see stresses in macrofibers (matrix is not shown on this picture).

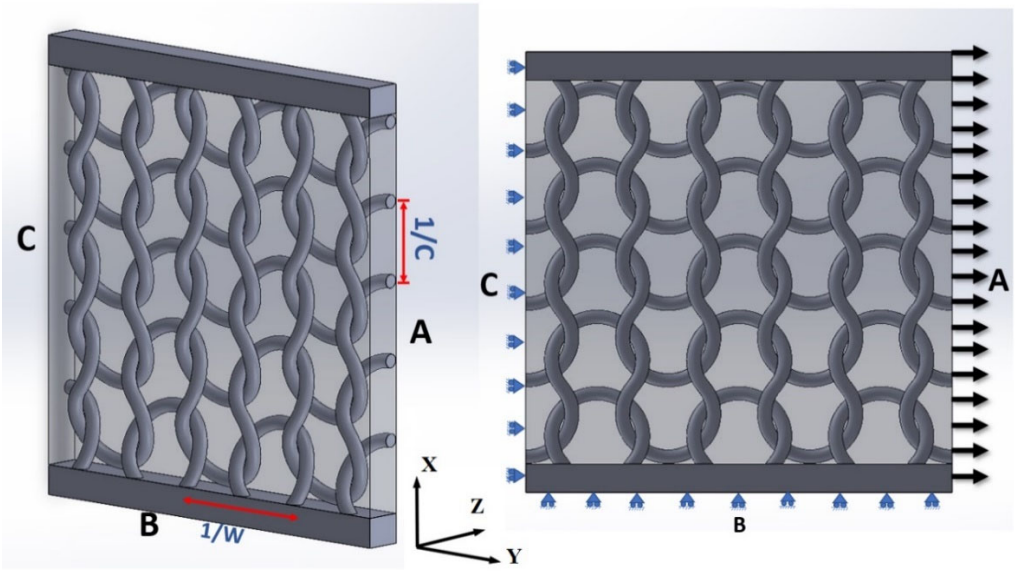

Figure 4. Boundary conditions for HCM volume with the frame.

 doi:10.20944/preprints202402.1294.v1

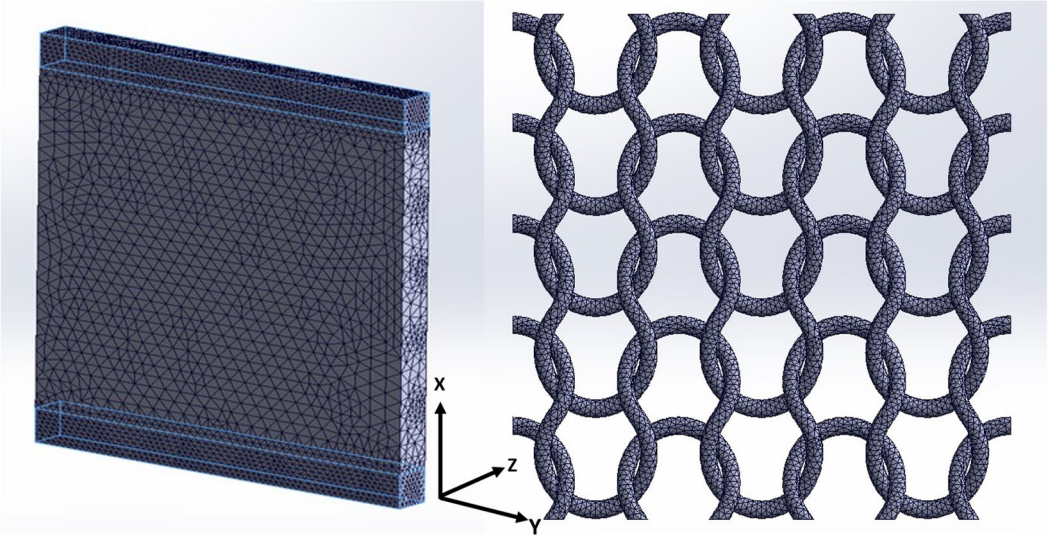

Figure 4. A. Mesh for HCM (Matrix and macrofiber) volume with the frame.

Applied external loads led to stress formation in every orthogonal cross-section of every macrofiber in the material. Calculations were carried out assuming that failure propagation is governing by threads failure. The deformations till rupture of the HCM matrix is much greater than those of the reinforcing macrofibers. The finite element method gives us detailed picture of internal stresses and deformations in the material. Our approach is focused on macrofibers rupture, matrix is working as a media transforming stresses between MF loops. Was found more heavily loaded macrofibers cross-section (with highest value of stretching normal stress along MF local longitudinal axes). According to periodical structure of loops in the fabric such cross-sections will be many. Within every repeating loop (repeating element) such cross-section will be one. If one of them fails, we will have one broken macrofiber surrounded by virgin loops (MF) within matrix. Ruptured macrofiber increases the overload on the closest macrofibers - neighbors in adjacent reinforcing fabric loops. More heavily loaded cross-sections in neighboring loops are dependent on applied external load orientation to the plate axis ***xy***. In every calculation they were recognized. Stress parameter which is used for characterization of the macrofiber overloading statement is averaged over crossection area stretching stress acting in the direction along the fiber in its current orthogonal cross-section. If we have two adjacent broken macrofibers plate was re-meshed and more heavily loaded cross-sections (locations of the cross-sections with highest value of the stress parameter) were found in the loops adjacent to the defect, consisting of two broken macrofibers. If we have three adjacent broken macrofibers, calculations show more heavily loaded cross-sections (position of the cross-sections) in the loops adjacent to the defect consisting of three broken macrofibers. In every such calculation, we are obtaining the stress parameter numerical values for maximally overloaded cross-sections. These calculations are possible to continue for defects with bigger size.

3.2. Calculations Using Model with a Frame

Curvature-based mesh was used for simulation, with maximal element SOLID 186 linear size equal to 0.1675 mm. Calculations were carried out using software ANSYS for all volume, and the results for normal stretching stresses (not averaged over cross-section area) in MF are shown in Figure 5. Stretching stress was calculated as:

$$\sigma_v(\eta,\xi) = \sigma_x l^2 + \sigma_y m^2 + \sigma_z n^2 + 2\tau_{yz} mn + 2\tau_{zx} nl + 2\tau_{xy} lm, \quad (1)$$

where σ_v is normal stress in the point of current orthogonal cross-section, σ_x is normal stress in the x-axis direction, σ_y is normal stress in the y-axis direction, σ_z is normal stress in the z-axis direction, τ_{yz} is shear stress in the yz plane, τ_{zx} is shear stress in the zx plane, τ_{xy} is shear stress in the xy plane, and l, m, n are direction cosines. Calculations were done combining ANSYS with MATLAB (for σ_v calculation).

 doi:10.20944/preprints202402.1294.v1

Stress distributions in every macrofiber internal cross-section's point were obtained, then locations of N orthogonal cross-sections for each macrofiber along its spatial geometrical line were selected and numbered. In every orthogonal cross-section, stress parameter - the average stretching stress value (across the cross-section's area) orthogonal to the cross-section's plane was calculated as follows:

$$<\sigma_v> = \frac{1}{S}\iint_0^S \sigma_v(\eta,\xi)dS \quad , \qquad (2)$$

where $<\sigma_v>$ is average normal stress in the cross-section, $\sigma_v(\eta,\xi)$ is local normal stress in different points of the fiber cross-section, η and ξ are coordinates in crossections plane, S is the area of the macrofiber cross-section.

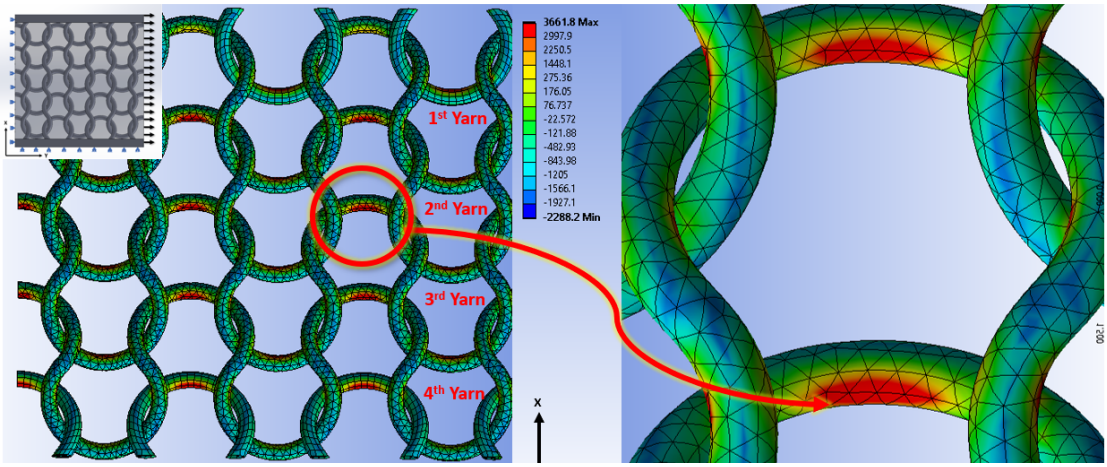

Figure 5. Local stretching stress (in MPa) orthogonal to each macrofiber orthogonal crossection in macrofibers inside the HCM plate. Simulation results.

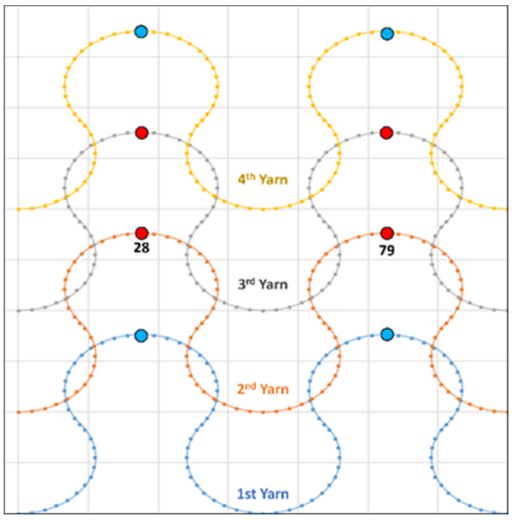

(**a**)

Preprints.org (www.preprints.org) | NOT PEER-REVIEWED | Posted: 23 February 2024 doi:10.20944/preprints202402.1294.v1

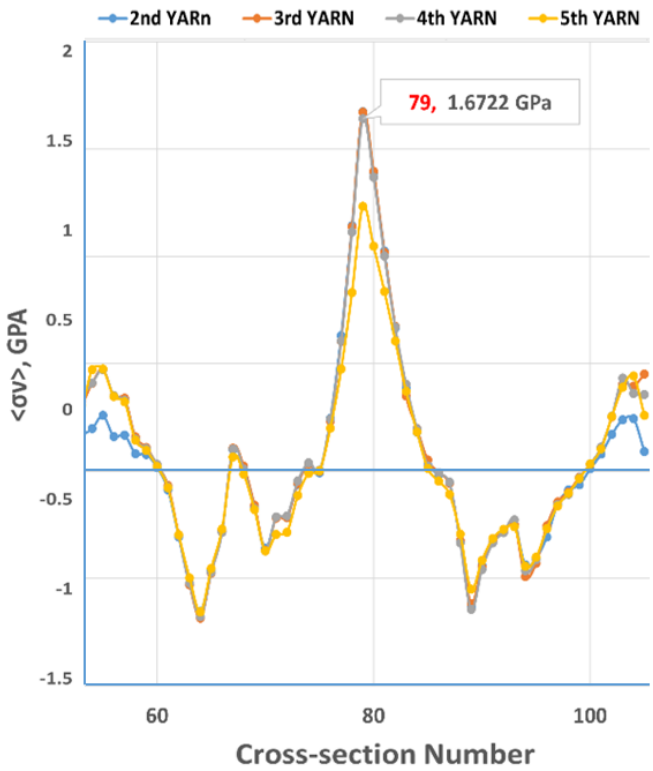

(**b**)

Figure 6. Stress parameter $<\sigma_v>$ values (averaged over MF cross-section's area normal stretching stress) in numbered cross-sections of 2nd, 3rd, 4th, and 5th MF in virgin material without broken MF: (a) numbered cross-sections location on the loops; (b) stress parameter values in numbered cross-sections along selected MF. Calculation was made for Matrix-Epoxy resin without OSA.

In virgin material, without broken macrofibers, according to the internal thread's architecture, local overstresses can be found in different macrofibers loop's places are shown in Figure 5 (scale is in MPa). Averaged over current cross-section areas local stretching stress $<\sigma_v>$ – stress parameter (SP) values in cross-sections along 2nd, 3rd, 4th, and 5th MF are shown in Figure 6. Looking on Figure 6a, it could be concluded - there is one more heavily stretched cross-section. In yarns 2, 3 and 4 (Figure 6), this is cross-section 79 (numbering is the same for every thread). Stress parameter values calculated along macrofibers are shown in Figure 6b. All other cross-sections are loaded with smaller overstress (have smaller value of the stress parameter). Crossections 28 in all threads have the same stress parameter as in 79. Small difference in calculated values is because vicinity of the plate borders. About cross-sections 28 and 79 in the fives thread. In virgin material with many threads (big size plate) stress parameter must be the same as in threads 2-4. Deviations are coming from vicinity of the plate's border in FEM calculations. Calculations shown, when we use representative volume having only one loop stress deviations in peak stress parameter values was bigger (with the same mesh).

Suppose the first thread breaks. According to our model, it will happen in one of the more heavily loaded cross-sections. In our situation, it will be cross-section 79 in the MF 3. It is worth to mentioning that the choice of the first broken cross-section is rather arbitrary, and it could be referred to the broken cross-section as the cross-section in a randomly chosen representative part of the material. Cross-section 79 in the MF 3 is stretched with the maximal normal stress with the SP value 1672.2 MPa. In the situation with pure epoxy resin matrix, the value is 1672.2 MPa, and in the situation with epoxy resin with 20% OSA, the value is 1679.0 MPa.

 doi:10.20944/preprints202402.1294.v1

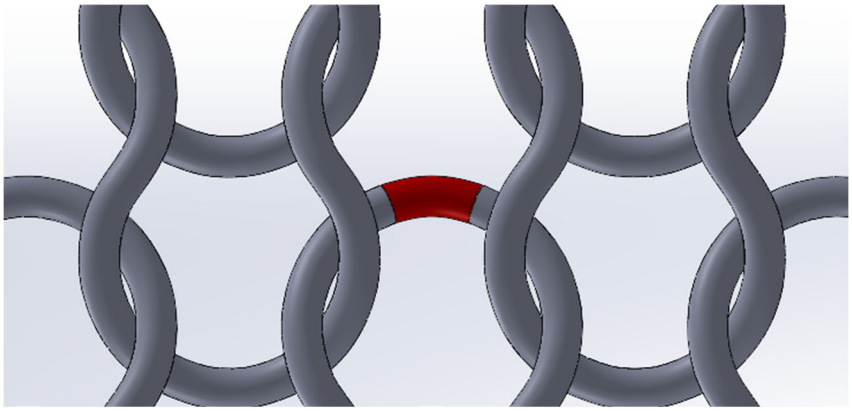

Figure 7. Location of the broken cross-section on third MF.

Further in calculations, the failed yarn's cross-section is simulated by a thin, soft, cylindrical insertion into the yarn body (small red part in the Figure 7), with an elastic modulus close to zero. This insertion, which has the same diameter as the yarn, models the location of rupture in the thread. An investigation of debonding between matrix and MF, as well as the internal delamination and fraying of the yarn (MF), is not included in the present research.

We placed the soft insertion in cross-section 79 of the yarn 3. Perfect bonding took place between the separate MF parts and the MF and matrix in the finite element model. Failure in the composite material led to the formation of overstresses on the cross-sections of the nearest neighbors in the vicinity of the ruptured place. Figure 8 shows stress parameter distribution in the plate with one rupture.

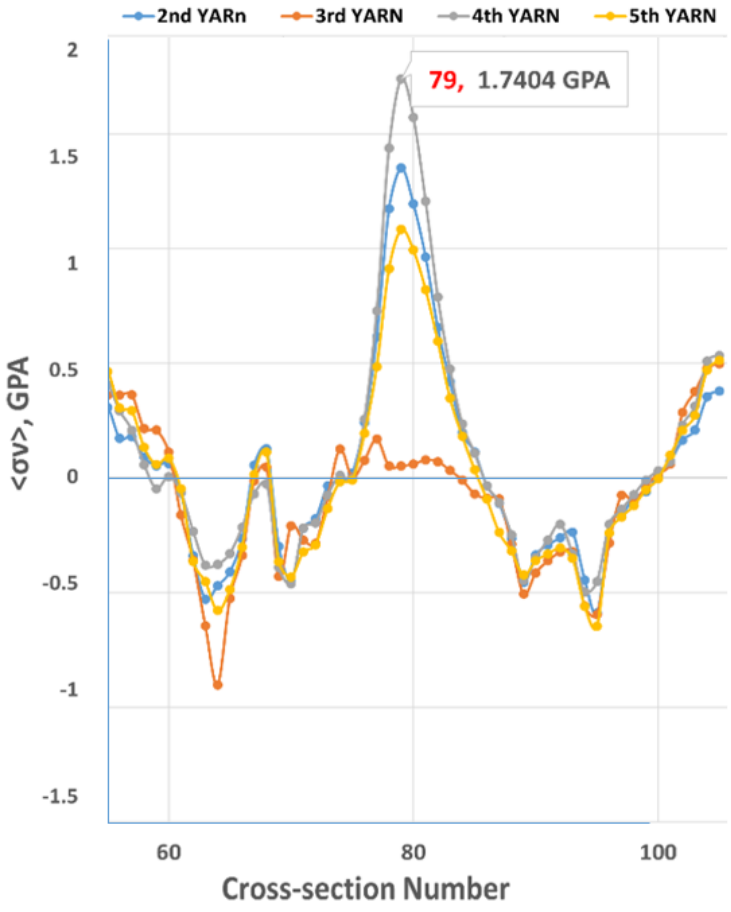

Figure 8. Cross-sections with maximal normal stresses (stress parameter $<\sigma_v>$) in material with one broken macrofiber. Cross-section 79 in the yarn 3 is broken. Epoxy resin matrix without OSA.

 doi:10.20944/preprints202402.1294.v1

Rupture is in the cross-section 79 in the MF number 3. More overloaded are crossections number 79 in the MF number 4 and 2. Stress parameter value in these cross-sections are equal to 1740.0 MPa (in MF 2 we obtained slightly smaller) for the case with epoxy matrix (without OSA) and 1748.0 MPa for the case with epoxy matrix having 20% OSA. It can be also observed that the stress value in the yarn 3 dropped nearly to 0 (in reality it is 0) when we added the soft inclusion. If cross-section 79 in the yarn 4, will fail, there would be two adjacent broken threads in the material, and these two breakages would form a defect consisting of two adjacent broken macrofibers (numbers 3 and 4). Threads forward (and back along the crack's line)) to the two ruptured macro-fibers will be more heavily overloaded.

Then, three adjacent broken MF, then four adjacent broken macrofibers were introduced in the plate (broken cross-sections were replaced by soft inclusions) and overloads on adjacent to broken macrofibers were calculated. (see Figure 9).

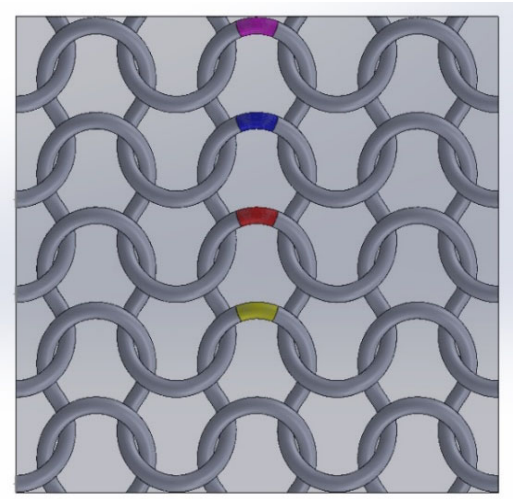

Figure 9. Broken cross-sections replaced by soft inclusions.

The deformation of the CM with epoxy matrix is shown in Figure 10. In Figure 10b broken ends of MF are forming empty "channels" in the matrix because of matrix elastoplastic properties.

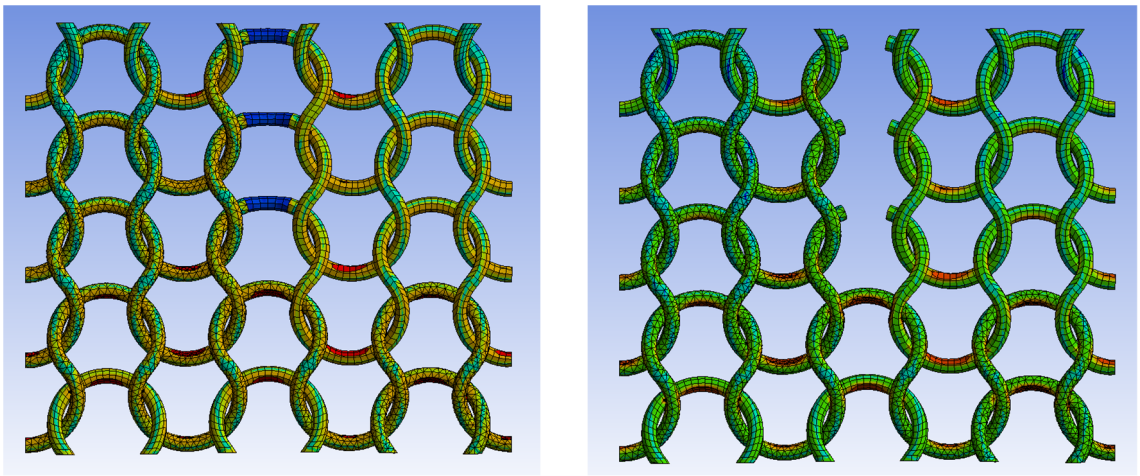

(**a**) (**b**)

Figure 10. FEM simulations (a) with and (b) without soft inclusions.

Maximal overstress in overstressed cross-sections in the vicinity of j broken fibers is shown in the Table 2. For four broken fibers plate border is significantly affect the result. Normal stress values are shown for calculations done using models with and without the frame, as well as for CM with epoxy matrix and epoxy matrix resin with 20% OSA. Looking on the data in the table, we see that

Preprints.org (www.preprints.org) | NOT PEER-REVIEWED | Posted: 23 February 2024 doi:10.20944/preprints202402.1294.v1

overstress values are slightly dependent on the addition of OSA to the Epoxy matrix. Higher dependence is possible to expect with very high OSA particles concentrations. Model geometry (with and without the frame) affects the failure scenario such way - without the frame, the model has slightly higher normal stress values comparing to the condition with the frame. The enlargement of observed broken threads (and number of loops) leads to a rapid increase in the numerical task size and calculation time. In order to address this situation, a linear approximation of the overstress dependence on the size of broken yarns clusters was accepted, as shown in Figure 11.

Table 2. Maximal tensile stress.

Break number	Stress parameter (normal stress) $<\sigma_i>$	Calculation without the frame (MPa), epoxy matrix resin with 0% OSA	Calculation without the frame (MPa), epoxy matrix resin with 20% OSA	Calculation with the frame (MPa), epoxy matrix resin with 0% OSA	Calculation with the frame (MPa), epoxy matrix resin with 20% OSA
Virgin material	σ_0	1755.9	1761.0	1672.2	1.679.0
1 break	σ_1	2354.5	2370.1	1740.0	1748.9
2 breaks	σ_2	2646.0	2690.1	1670.9	1679.1
3 breaks	σ_3	2642.5	2687.2	1365.7	1369.2
4 breaks	σ_4	1700.3	1820.1	-	-

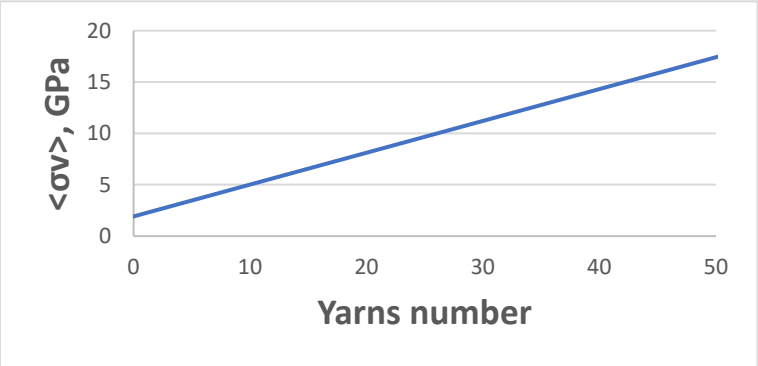

Figure 11. Maximal tensile stress parameter $<\sigma_v>$ on the nearest yarns-neighbors on the border of the cluster consisting of ***i*** broken yarns (MF).

4. Model of Damage Accumulation in the CMHR

4.1. Material Failure Probability Modeling

As shown in Figures 3,4 and 12a we can easily represent our material as a "chain of bundles". The whole plate consists of ***M*** chain sections. Yarns loops (MF) in the plate between two crossections ***A*** and ***B*** (see Figure 12a,b) represents one section of a chain, and in the same time each ***C***-shape curved loop part, each oriented approximately in the direction parallel to the external stretching, can be observed as the bundle element. Each bundle consists of ***N*** elements, where ***N*** is the number of loops in the orthogonal cross-section of the stretched composite plate (***N***=5 in Figure 12a). The ***S***-shape part in each loop, participating in the material's common integrity, does not participate in material failure under applied load (transparent blue in Figure 12a). These MF segments are easily stretched or, in some cross-sections, compressed. In the cross-section ***A***, the overstress parameter value $<\sigma_v>$ is reaching ***80***% of the maximal overstress value between cross-sections ***A*** and ***B***. The same for the cross-section ***B*** (see Figure 13). The length of the MF segment (along the loop) between cross-sections ***A***

 doi:10.20944/preprints202402.1294.v1

and $\boldsymbol{B}$ is designated as δ_L, what is the length of the bundle in our model. Composite loading by tension leads to diffuse MF breakage accumulation. Isolated single MF break is associated with one element failure in the community of $\boldsymbol{M} \times \boldsymbol{N}$ elements. All elements have the same dimensions; geometrically, each element involves a MF piece between two orthogonal crossections $\boldsymbol{A}$ and $\boldsymbol{B}$ with length δ_L surrounded by a matrix.

$W(\sigma)$ -is the probability of a single element rupture.

4.2. Damage Accumulation

Modeling damage accumulation in stretched CM reinforced by weft-knitted fabric assumes, that failure is a complex stochastic process that starts with scattered, isolated breaks accumulation in MF sections, redistributing overstresses on adjacent to broken virgin MF, rupture of overstressed neighbors and formation of broken MF clusters. Clusters are growing inside the bundles; each bundle is orthogonal to the applied stretching direction. This process starts. At beginning, if we have only small size clusters is necessary to increase applied force value for obtaining bigger clusters. Clusters are growing. Process will transform to ultimate catastrophic biggest cluster growth (when we have such) with very small increase of applied load leading to next cluster formation. Growth happened because the overstress distributed on the closest unbroken neighbors will practically immediately initiate a segment break in the adjacent MF. In the framework of this model, we neglected the interaction of clusters between two adjacent bundles.

We can introduce one *random variable* $\boldsymbol{J}(\sigma)$ - size of the cluster, with the probability function $P\{\boldsymbol{J}(\sigma) \geq i\}$. $P\{\boldsymbol{J} \geq \boldsymbol{i}\}$ *is the probability to* find a cluster consisting of at least $\boldsymbol{i}$ adjacent (in one bundle) broken MF when the externally applied tensile stress reaches σ and stress parameter value on MF σ_0 . It is obvious that

P(j=1) $=W(\sigma_0)$.

The probability of find a cluster consisting of at least two adjacent broken MF is $P(j\geq 2) = P(j=1)(1-(1-W(\sigma_1))^2)$.

Here we want to show, that cluster consisting of at least two adjacent broken MF is forming by failure of one of the nearest neighbors to rupture place on the broken MF. Two neighbors are similarly overloaded on the border of the cluster consisting of one broken MF (see Figure 8). Suppose broken is crossection 79 belonging to the yarn 2, two neighbors (crossections 79 in 1st yarn and 79 in 3th yarn become overloaded). Stress parameter value in this crossections become equal to σ_1.

The probability of finding a cluster consisting of at least three adjacent broken MF is

$P(j\geq 3) = P(j \geq 2)(1-(1-W(\sigma_2))^2)$, because two neighbors are similarly overloaded on the border of the cluster consisting of two broken MF. (in Figure 6 a, cross-sections 79 belonging to yarns 1 and 4, if broken crossections are number 79 in yarns 2 and 3). The probability of finding a cluster consisting of at least four adjacent broken yarns is

 doi:10.20944/preprints202402.1294.v1

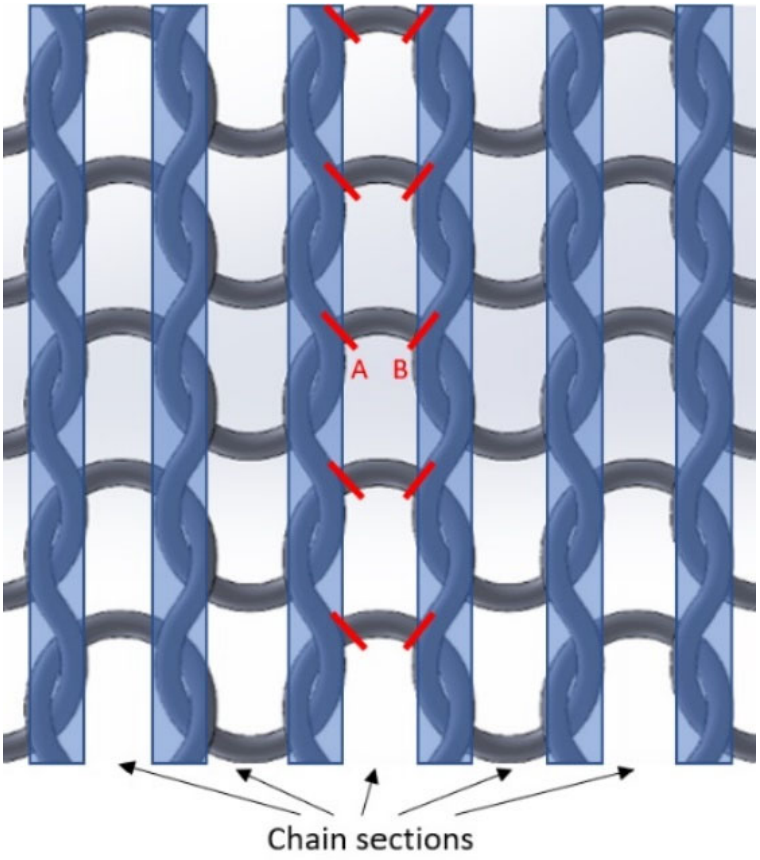

(**a**)

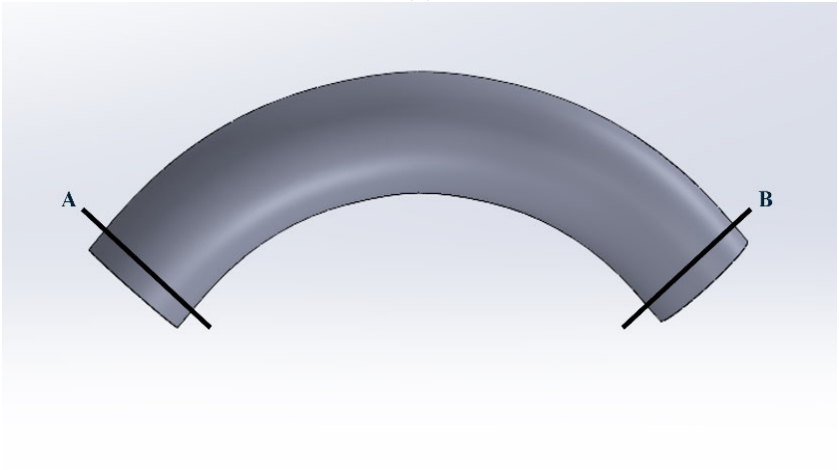

(**b**)

Figure 12. a) .chain of bundles. **b** Repeating yarn element in the geometric model of chain of bundles.

$P(j\geq4) = P(j\geq3)\,(1-(1-W(\sigma_3))^2)$.

The probability of finding a cluster consisting of at least five adjacent broken yarns is equal to $P(j\geq5) = P(j\geq4)\,(1-(1-W(\sigma_4))^2)$, because two neighbors are similarly overloaded on the border of the cluster consisting of four broken yarns. Continuing this procedure, we can calculate the probability of finding clusters consisting of at least $\boldsymbol{i}$ adjacent broken MF under applied external stress σ:

$P(j\geq i) = P(j\geq i-1)\,(1-(1-W(\sigma_{i-1}))^2)$.

Preprints.org (www.preprints.org) | NOT PEER-REVIEWED | Posted: 23 February 2024 doi:10.20944/preprints202402.1294.v1

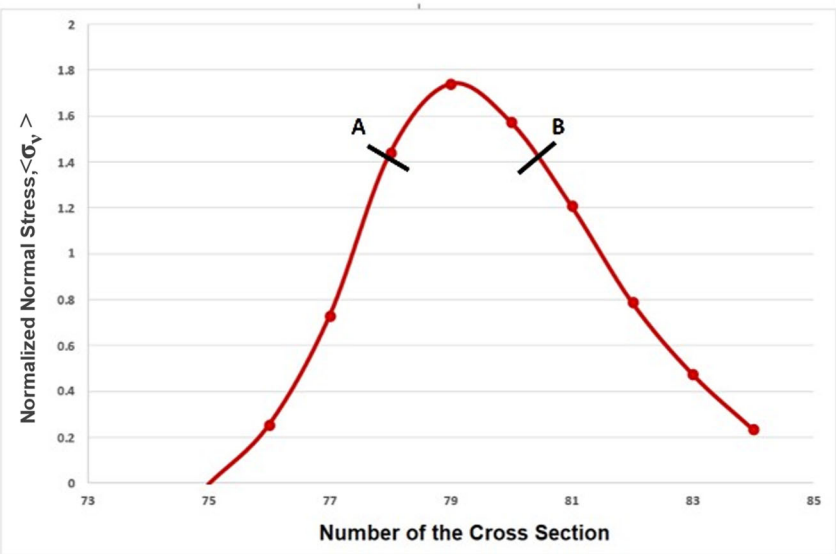

Figure 13. Stress parameter <σν > values distribution along the overloaded MF element in the chain of bundles model. Between crossections A and B MF is loaded by stress values.

$\sigma_0 \in [\sigma\text{-}20\%\sigma;\ \sigma\text{+}20\%\sigma]$. This part starts from crossection ***A*** to crossection ***B*** (see Figure 12).

5. Numerical Example

Numerical calculations were done for HCM - Epoxy resin matrix with 20% OSA reinforced by Basalt fiber weft-knitted fabric. Distribution of single loaded element strength is a typical lowest values distribution [28–33]. Weakest elements strength distribution was accepted in Weibull form:

$$W(\sigma) = 1 - \exp\left(-\frac{L}{\delta_L}\left(\frac{\sigma}{\sigma_A}\right)^{\beta}\right) = 1 - \exp\left(-\left(\frac{\sigma}{\sigma_C}\right)^{\beta}\right), \quad (3)$$

Were $\sigma_A, \sigma_C, \beta$ are constants.

Traditionally, for unidirectional CM parameters σ_C, β are characterizing single microfiber. Numerical values for them are possible to obtain performing single fiber fragmentation test. Unfortunately, this approach is not convenient for our macrofibers. In modelling we accepted numerical values of the parameters: $\sigma_C = 1.2\ GPa$ and $\beta = 3$. The numerical simulation results are shown in Figure 14. Is possible to see, that with increased of the cluster size, probabilistic curves link together forming one common envelope. That means that the next failure on the border of the cluster will occur practically immediately, without an increase in the external load. Crack is becoming unstable. This is the probability curve to find in the plate infinity big crack (in reality, crack which is crossing plate's orthogonal crossection). Multiplying the number of elements ($\boldsymbol{N\ x\ M}$) in one particular plate with the probability functions $P\{J(\sigma) \geq \boldsymbol{i}\}$, we can obtain predicted different size clusters in HCM material volume, starting with single MF breaks until unstable cluster formation. Performed numerical modelling shown slightly higher all size defects concentration values in the plate with the size: width 420 mm, height 400 mm, and thickness 2.43 m in CMHR situation with 20% OSA comparing with material without OSA. Difference in the stress value for unstable crack formation is small between mentioned CMHR plates.

 doi:10.20944/preprints202402.1294.v1

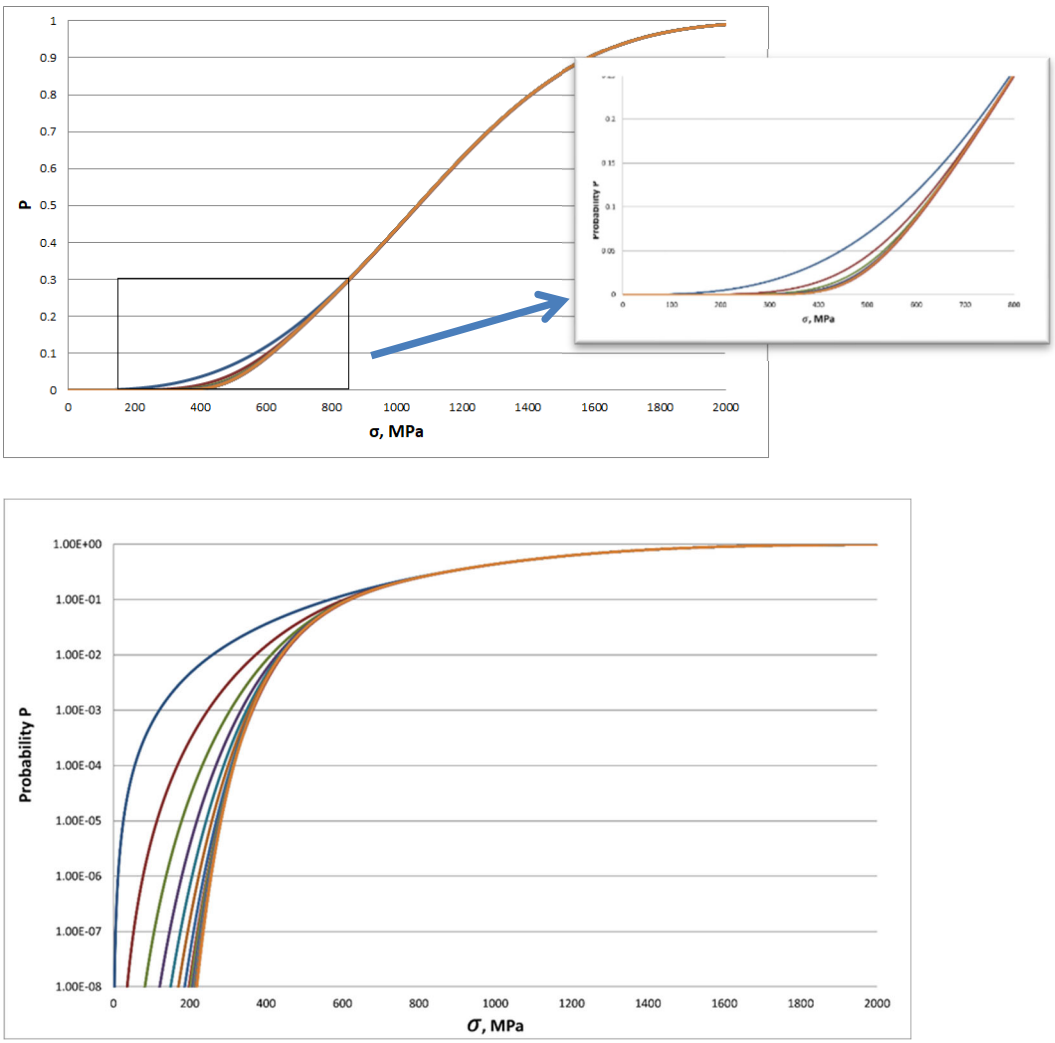

Figure 14. Probability of finding clusters consisting of at least i adjacent broken yarns in stretched material.

6. Conclusions

The present research is focused on experimental and numerical damage accumulation processes investigation (under mechanical tension) in HCM made of epoxy resin, Oil Shale Ash (0% or 10%, 20%) and basalt fiber textile reinforcement.

Epoxy resin samples with 0% or 10%, 20% amount of OSA were fabricated and elastic properties of them were experimentally measured. Was obtained Young modulus value increase for 13% between Epoxy matrix and Epoxy with 20% OSA matrix. At the same time impregnated Basalt fiber thread Young modulus increased only for 1,1%.

Textile reinforcement was modelled as a 3D structure consisted of macrofibers (impregnated threads) in the hybrid matrix. Numerical, based on textile reinforcement topology FEM model was created for stresses calculations. Optimizing calculations precision (mech density) and single task calculation time, model with five by five reinforcing textile loops was chosen for realization.

Were obtained overstress values in the HCM in situation when few macrofibers break. Obtained calculated overstress values were sensitive to the number of broken MF. Situation was slightly improved using numerical model with the "frame" (introduced in FEM calculations plate parts with averaged elastic properties).

Probabilistic structural numerical model was created. Model predicts number of different sizes clusters formation in the HCM subjected to stretching. Cluster is a few adjacent broken macrofibers (yarns). Increase of external stress is leading to bigger clusters formation in the material till one cluster

 doi:10.20944/preprints202402.1294.v1

(non-stable crack) is separating HCM plate on parts. Only overstressed parts of the textile loops – 3.8% of every loop length is participating in single breaks accumulation process (overstressed from 80% to 100% of the maximal value) realizing in the textile reinforcement.

Modelling allows to predict whole different size clusters formation process in loaded HCM with textile reinforcement consisting of NxM loops. Damage accumulation (all size clusters formation) happens more intensively in CMHR with 20%OSA comparing with CMHR without OSA, at the same time this difference is small.

Author Contributions: Conceptualization, O.K. and A.K.; methodology, O.K., A.K., I.L., I.N., R.M., and M.V.; validation, U.H.V., A.M., K.R.K., and I.J.; formal analysis, O.K., A.M., and A.K.; investigation, I.J., U.H.V., and K.R.K.; resources, A.K.; original draft preparation, O.K., A.K., and U.H.V.; review and editing, A.K. and I.N.; supervision, O.K. and A.K.; funding acquisition, A.K. All authors have read and agreed to the published version of the manuscript.

Funding: The authors acknowledge financial support from the Baltic Research Programme, project no. EEA-RESEARCH-165 "Innovation in concrete design for hazardous waste management applications" under the EEA Grant of Iceland; Liechtenstein and Norway Project contract no. EEZ/BPP/VIAA/2021/6.

Institutional Review Board Statement: Not applicable.

Informed Consent Statement: Not applicable.

Data Availability Statement: All data are presented in the paper.

Conflicts of Interest: The authors declare no conflicts of interest.

Abbreviations:

Symbol	*Notation*
j	defect size (number of adjacent broken macrofibers)
σ_v	stress in the internal point of the macrofiber, acting along the normal vector to current crossection
$<\sigma_v>$	Stress parameter - average, across the cross-section's area, stretching stress value normal to the current cross-section's plane
$J(\sigma)$	Random variable – cluster's size
$P\{J \geq i\}$	*probability to* find cluster in one bundle, consisting of at least i adjacent broken macrofibers
Terminology	Explanation
OSA	*oil shale ash*
HCM	*hybrid composite material - epoxy+OSA+textile reinforcement*
microfiber	*Basalt microfiber 13-16 μm in diameter*
yarn, thread	*group of microfibers (250 microfibers)*
Macrofiber (MF)	*group of slightly twisted microfibers (250 microfibers) impregnated with epoxy resin with OSA particles. Approx. diameter 0.55 mm -1mm*
bundle	*series of adjacent macrofibers parts (impregnated yarns) in the plane orthogonal to loading direction. MF parts belongs to different loops in the textile. Length of different MF part in the bundle is the same for all MF parts (belonging to different loops) and depends on stretching stress distribution in loops*
cluster	*Group of broken adjacent MF*

References

1. Hardaker M. and Richardson M. O. W. Trends in Hybrid Composite Technology, *Polymer-Plastics Technology and Engineering* (1980) - Issue 2K., 15:2, 169-182, DOI: 10.1080/03602558008070011
2. Jerzynska A. and Egner H. Energy Equivalence Based Estimation of Hybrid Composites Mechanical Properties, *Materials* (2023), 16, 4215. https://doi.org/10.3390/ma16124215 (Open access).
3. Atmakuri A., Palevicius A., Vilkauskas A. and Janusas G. Review of Hybrid Fiber Based Composites with Nano Particles—Material Properties and Applications, *Polymers* (2020), 12, 2088; doi:10.3390/polym12092088 (Open access).
4. Aveston J. and Sillwood J. M. Synergistic fibre strengthening in hybrid composites, *Journal of Materials Science*, 11, 1877–1883 (1976). https://doi.org/10.1007/BF00708266
5. Radulović J. Hybrid Filament-wound Materials: Tensile Characteristics of (Aramid Fiber/Glass Fiber)-Epoxy Resins Composite and (Carbon Fibers/Glass Fiber)-Epoxy Resins Composites, *Scientific Technical Review*, (2020), Vol.70, No.1, pp.36-46. doi: 10.5937/str2001036R
6. Sim J., Kang Y., Kim B. J., Park Y. H. and Lee Y. C. Preparation of Fly Ash/Epoxy Composites and Its Effects on Mechanical Properties, *Polymers* 2020, 12(1), 79; https://doi.org/10.3390/polym12010079 (Open access).
7. Kononova O., Krasnikovs A., Kharkova G., Zalesky J. and Machanovsky E. Mechanical Properties Characterization by Inverse Technique for Composite Reinforced by Knitted Fabric. Part 1. Material Modeling and Direct Experimental Mechanical Properties Evaluation. *Journal of Vibroengineering*, ISSN 1392 – 8716, June - Vol.14, Iss.2. (2012) p. 681-690.
8. Ogin S. Textile-reinforced composite materials. Technology & Engineering. *In Handbook of Technical Textiles*, Ed. A R Horrocks, Subhash C. Anand, Chapter 11. 2000, p. 265-280.
9. Mobasher B. Mechanics of Fiber and Textile Reinforced Cement Composites, CRC Press, 473 p. ISBN-10: 1439806608
10. Katerelos, D.T.G., Krasnikovs, A., Varna, J. Variational models for shear modulus of symmetric and balanced laminates with cracks in 90-layer International. *Journal of Solids and Structures*, 2015 71, pp. 169-179 (Open Access).
11. Pakkam Gabriel V.R., Loukil, M.S., Varna J. Analysis of intralaminar cracking in 90-plies of GF/EP laminates with distributed ply strength. *Journal of composite materials* 55 (26), 3925-3942
12. Varna, J., Berglund, L.A., Krasnikovs, A., Chihalenko, A. Crack opening geometry in cracked composite laminates. International *Journal of Damage Mechanics* 1997, 6(1), pp. 96-118.
13. Bogenfeld, R., Kreikemeier, J., Wille, T. Review and benchmark study on the analysis of low-velocity impact on composite laminates. *Engineering Failure Analysis*, Volume 86, April 2018, Pages 72-99.
14. J. Jefferson, A., Sivakumar M.Srinivasan, Arockiarajan, A., Hom Nath Dhakal. Parameters influencing the impact response of fiber-reinforced polymer matrix composite materials: A critical review *Composite Structures* V.224, 15 September 2019, 111007.
15. Pandita S.D., Falconet D., Verpoest I. Impact properties of weft knitted fabric reinforced composites *Composites Science and Technology*. V.62, I.7–8, June 2002, Pages 1113-1123.
16. Krasnikovs A., Kononova O., Machanovskis A., Zaharevskis V., Akishins P. and Ruchevskis S. Mechanical Properties Characterization for Composite Reinforced by Knitted Fabric using Inverse Technique. Part 2. Mechanical properties experimental evaluation by frequency eigenvalues method// *Journal of Vibroengineering*, ISSN 1392 – 8716, June Vol.14, Iss.2. (2012) p. 691-698.
17. Lee, M., Mata-Falcón, J. & Kaufmann, W. Load-deformation behaviour of weft-knitted textile reinforced concrete in uniaxial tension. *Mater Struct* 54, 210 (2021). https://doi.org/10.1617/s11527-021-01797-5
18. Jacobsen A. J., Luo J. J. and Daniel I. M. Characterization of constitutive behavior of satinweave fabric composite. *J. Composite Materials*, Vol. 38, No. 7, pp. 555-565, 2004.
19. Abot J. L., Yasmin A., Jacobsen A. J. and Daniel I. M. "In-plane mechanical, thermal, and viscoelastic properties of a satin fabric carbon/epoxy composite," *Composites Science and Technology*, Vol. 64, pp. 263-268, 2004.
20. Mallick P. Composites Engineering Handbook. New York: Marcel Dekker, Inc. (1997).
21. Kononova O., Krasnikovs A., Dzelzitis K., Kharkova G., Vagel A., Eiduks M. Mechanical properties modeling and experimental verification for cotton knitted fabric composites, *Estonian Journal of Engineering*, vol.17, issue 1, 2011, p.39-50.
22. Znoaga M., Tanasa F. Complex textile structures as reinforcement for advanced composite materials. *International conference of scientific paper* AFASES (2014).

23. Morgan, P. (2005). Carbon Fibers and Their Composites (1st ed.). CRC Press. https://doi.org/10.1201/9781420028744
24. Hu J. Introduction to three-dimensional fibrous assemblies. In J. Hu, 3-D fibrous assemblies Properties, applications and modelling of three-dimensional textile structures, Cambridge: Woodhead Publishing (2008).
25. Huang Zh., Zhang Y. and Ramakrishna S. Modeling of the progressive failure behavior of multilayer knitted fabric-reinforced composite laminates, *Composite Science and Technology*, v. 61, Issue 14, November 2001, p. 2033–2046.
26. Ramakrishna S. Tensile Properties of Plain Weft Knitted Glass Fiber Fabric Reinforced Epoxy Composites, *Journal of Reinforced Plastics and Composites*, July 1997 vol. 16 no. 10 946-966, doi: 10.1177/073168449701601005.
27. Rios C.R., Ogin S.L., Lekakou C. and Leong K.H. The Relationship Between Fibre Architecture and Cracking Damage in a Knitted Fabric Reinforced Composite, http://www.iccm-central.org/Proceedings/ICCM12proceedings/site/ papers/ pap1035.pdf
28. Hansen A. The Three Extreme Value Distributions: An Introductory Review, *Frontiers in Physics*, 10 Dec. 2020, *Sec. Interdisciplinary Physics*,Vol. 8 – 2020, https://doi.org/10.3389/fphy.2020.604053.
29. Engelbrecht-Wiggans AE, Phoenix SL. Comparison of maximum likelihood approaches for analysis of composite stress rupture data. *J Mater Sci.* (2016), 51:6639–61. doi: 10.1007/s10853-016-9950-3
30. Mahesh S, Phoenix SL, Beyerelin IJ. Strength distributions and size effects for 2D and 3D composites with Weibull fibers in an elastic matrix. *Int. J Fract.* (2002) 115:41–85. doi: 10.1023/A:1015729607223.
31. Sutherland L. S. and Guedes Soares C. Review of probabilistic models of the strength of composite materials. *Reliability Engineering and System Safety* 56 (1997) 183-196, 1997 Elsevier, doi.org/10.1016/S0951-8320(97)00027-6.
32. Korabelnikov Yu. G., Tamuzh V. P., Siluyanov O. F., Bondarenko V. M. and Azarova M. T. Scale effect of the strength of fibers and properties of unidirectional composites based on them. *Mechanics of Composite Materials,* 20, pages 129–134 (1984)
33. Gutans J. and Tamuzh V. Scale Effect of the Weibull Distribution of Fibre Strength, *Mechanics of Composite Materials*, Vol. 6, 1984, pp. 1107-1109.
34. A. K. Kaw Mechanics of composite materials, Taylor & Francis, ISBN 0-8493-1343-0, Mechanical engineering series, 457 p., 2006.